Electronic supplementary materials *Mendeleev Commun.*, 2024, **34**, 481–483

Stabilization of the perovskite phase of $CsPbI_3$ with isonipecotic acid

Nadezhda N. Dremova, Gennady V. Shilov, Pavel A. Troshin and Lyubov A. Frolova

Content

Materials and methods S2

Figures S1. Tauc plots for $CsPbI_3$+x%INPA films of various compositions used for Eg estimation (assuming direct bandgap) S3

Figure S2. SEM image of the perovskite film $CsPbI_3$+30%INPA..... S3

Figure S3. Grain size distribution of the perovskite films: pristine, $CsPbI_3$+5% INPAI, $CsPbI_3$+10% INPA, $CsPbI_3$+15% INPA, and $CsPbI_3$+30% INPA S4

Figure S4. Evolution of the open circuit voltage (V_{OC}) (a), short circuit current density (J_{SC}) (b), and fill factor (FF); (c) values of the devices depending on the INPA loading in the $CsPbI_3$ films..... S5

Figure S5. Absorption spectra of the pristine $CsPbI_3$ film before and after light soaking at 500 mW/cm^2 and 35 ± 2 °C for 12 h in an inert atmosphere S6

Figure S6. Evolution of the normalized open circuit voltage (V_{OC}) (a), short circuit current (J_{SC}) (b), and fill factor (FF); (c) values of the devices depending on the INPA content in the $CsPbI_3$ films during 1400 h exposure under continuous light soaking (500±10 mW/cm^2, T= 35±2ºC)..... S7

Table S1. Optical absorption edges (and bandgaps) estimated from the Tauc plots for the $CsPbI_3$+x%INPA films with various compositions. S8

Table S2. Peak position of the photoluminescence for the $CsPbI_3$+x%INPA films with various compositions S8

Table S3. Average and the best (in brackets) values of power conversion efficiency (PCE), open-circuit voltage (V_{OC}), short-circuit current density (J_{SC}), and fill factor (FF) for the devices with different INPA contents S8

References S9

Materials and methods

Preparation of the perovskite films

Glass substrates were cleaned with deionized water, acetone, and isopropyl alcohol and sonicated followed by the RF-air plasma treatment for 5 min. The $CsPbI_3$ films with the varying INPA content ranging from 0 to 30 mol.% were deposited by a spin-coating method from a 0.625 M precursor solution containing equimolar amounts of CsI and PbI_2 dissolved in a mixture of N,N′-dimethylformamide (DMF)/dimethyl sulfoxide (DMSO) (7:1) followed by annealing at 140ºC for 1 min.

Characterization of the perovskite films

The X-ray diffraction patterns were obtained using a Bruker D8 diffractometer with the CuKα source. The UV-vis absorption spectra of the films were obtained using an AvaSpec-2048-2 fiber spectrometer integrated into a glove box. The PL spectra were measured in an inert atmosphere using an Ocean Insight QE Pro spectrometer with a 472 nm laser as an excitation source.

Perovskite Solar Cells Fabrication and Characterization

The perovskite solar cells were fabricated in the n-i-p structure: ITO/SnO_2/PCBA/$CsPbI_3$+x%INPA/PTA/VO_x/Al. The ITO-coated glasses (Kintec, 15 Ω sq^{-1}) were cleaned with deionized water, acetone, and isopropyl alcohol and sonicated for 10 min. The compact SnO_2 layer was deposited by spin-coating from commercial SnO_2 ink (15 wt/wt % SnO_2 colloidal dispersion in H_2O, Alfa Aesar Co.) at 3000 rpm for 20 s followed by annealing at 135°C for 15 min in air. All subsequent procedures were carried out in an inert atmosphere. For this purpose, the substrate with deposited tin oxide was transferred inside the MBraun glove box under an inert atmosphere of pure nitrogen (concentration of O_2 and H_2O <1 ppm). To passivate the surface of the oxide electron transport layer, a solution of phenyl-C61-butyric acid (PCBA) in chlorobenzene (0.1 mg mL^{-1}) was deposited at 3500 rpm for 30 s followed by annealing at 110°C for 15 min. The perovskite films were grown as described above. The INPA content in the absorber films was varied from 1 to 15 mol.% The PTA (poly[bis(4-phenyl)(4-methylphenyl)amine]) layer used as a hole-transport material was deposited by spin-coating of the solution in chlorobenzene (6 mg/mL) at 1000 rpm for 30 s. Finally, the device structure was completed by the thermal vacuum evaporation of a hole-selective interfacial layer of VO_x (99.6%, Aldrich) (30 nm) and 120-nm thick aluminum electrodes. The active surface area of the solar cells ranged from 0.2 to 0.3 cm^2. The solar cells were characterized by I-V and EQE measurements as reported previously.[S1]

Study of the photostability of perovskite films and devices

The aging experiments were performed using special setups installed inside the MBraun glove box filled with pure nitrogen (O_2, H_2O <0.1 ppm) under continuous illumination with a power of 500±10 mW/cm^2 at temperature 35±2 ºC.

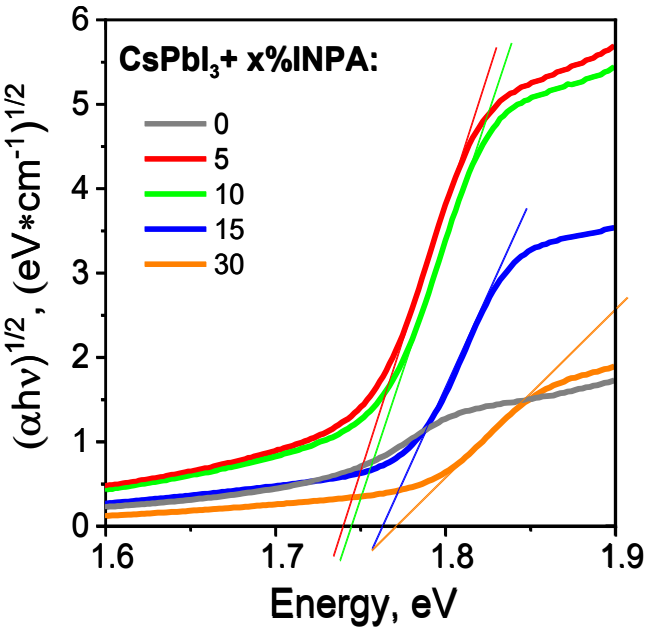

Figure S1. Tauc plots for the $CsPbI_3$+x%INPA films of various compositions used for E_g estimation (assuming a direct bandgap).

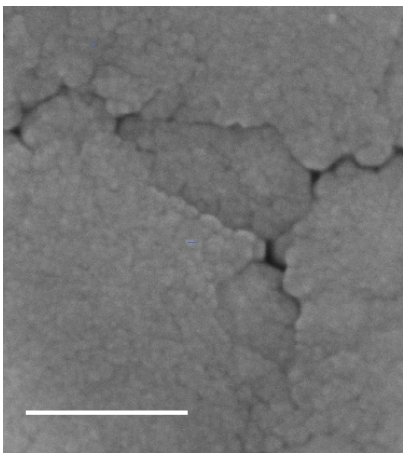

Figure S2. SEM image of the $CsPbI_3$+30% INPA perovskite film.

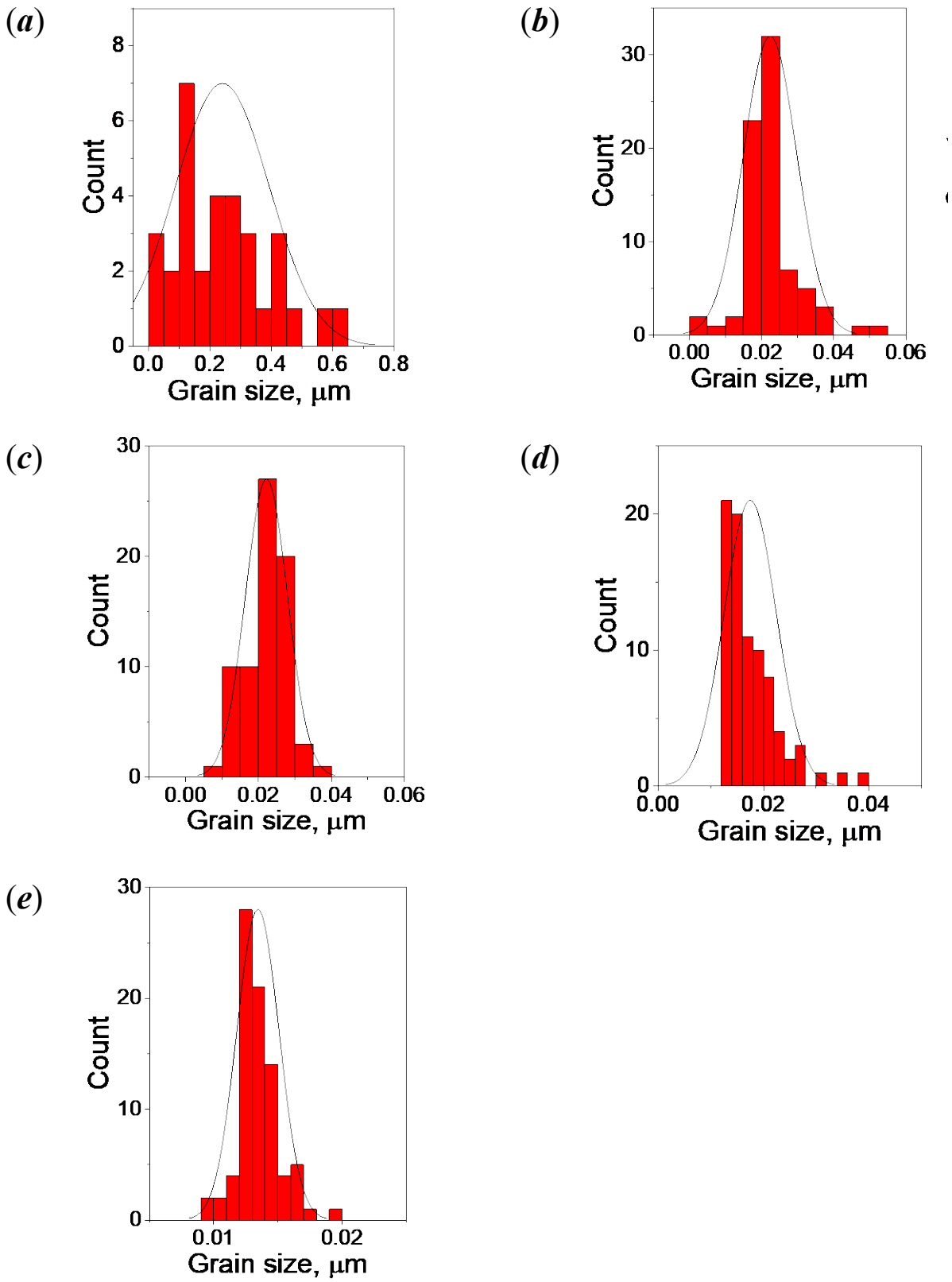

Figure S3. Grain size distribution for the pristine $CsPbI_3$ (***a***), $CsPbI_3$+5% INPAI (***b***), $CsPbI_3$+10% INPAI (***c***), $CsPbI_3$+15% INPA (***d***), and $CsPbI_3$+30% INPA (***e***) perovskite films.

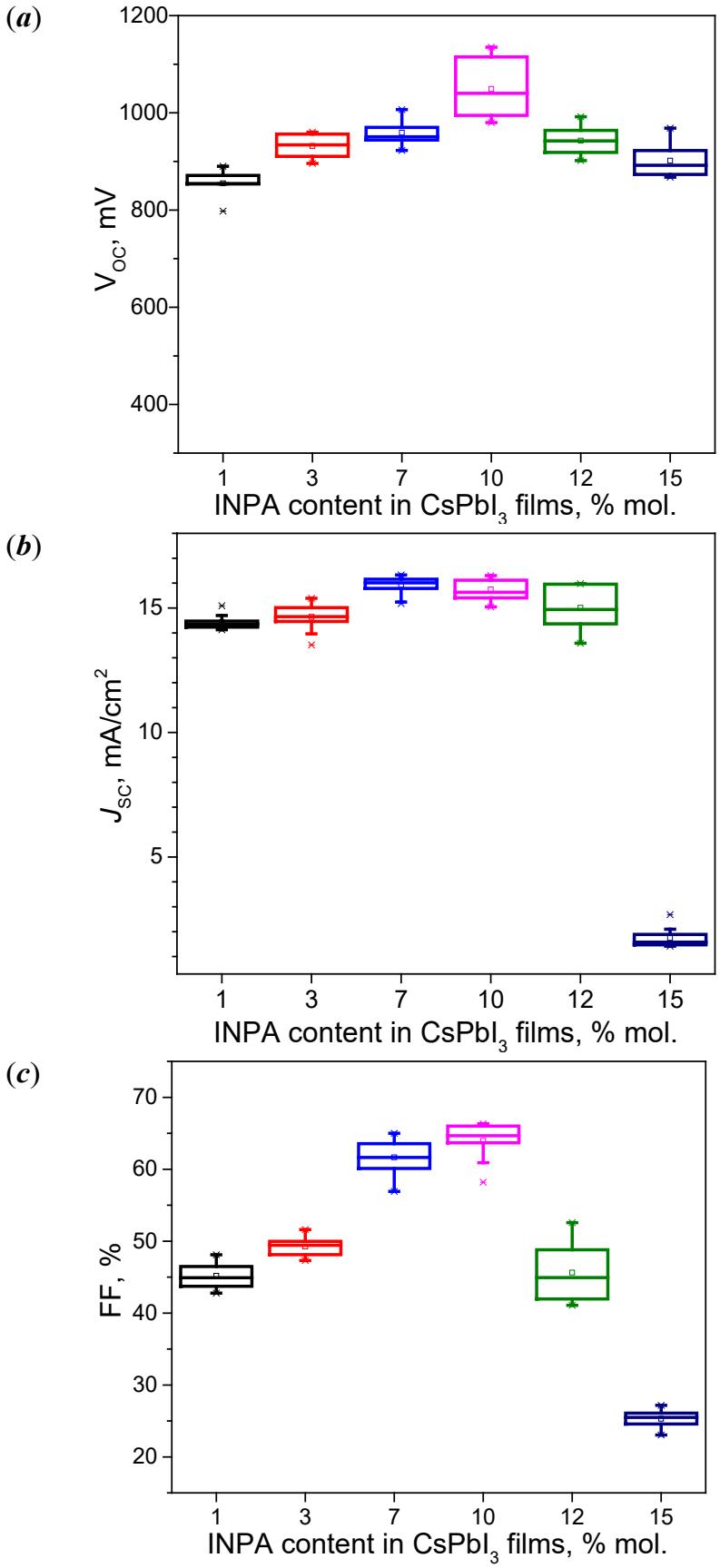

Figure S4. Evolution of the open circuit voltage (V_{OC}) (***a***), short circuit current density (J_{SC}) (***b***), and fill factor (FF) (***c***) values of the devices depending on the INPA loading in the $CsPbI_3$ films.

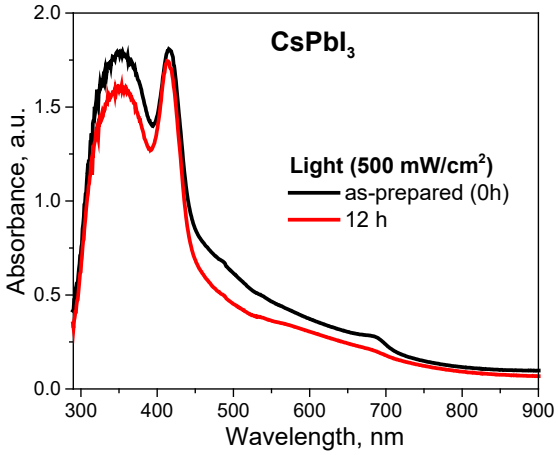

Figure S5. Absorption spectra of the pristine $CsPbI_3$ film before and after light soaking (500 mW/cm^2, 35 ± 2 °C) for 12 h in an inert atmosphere.

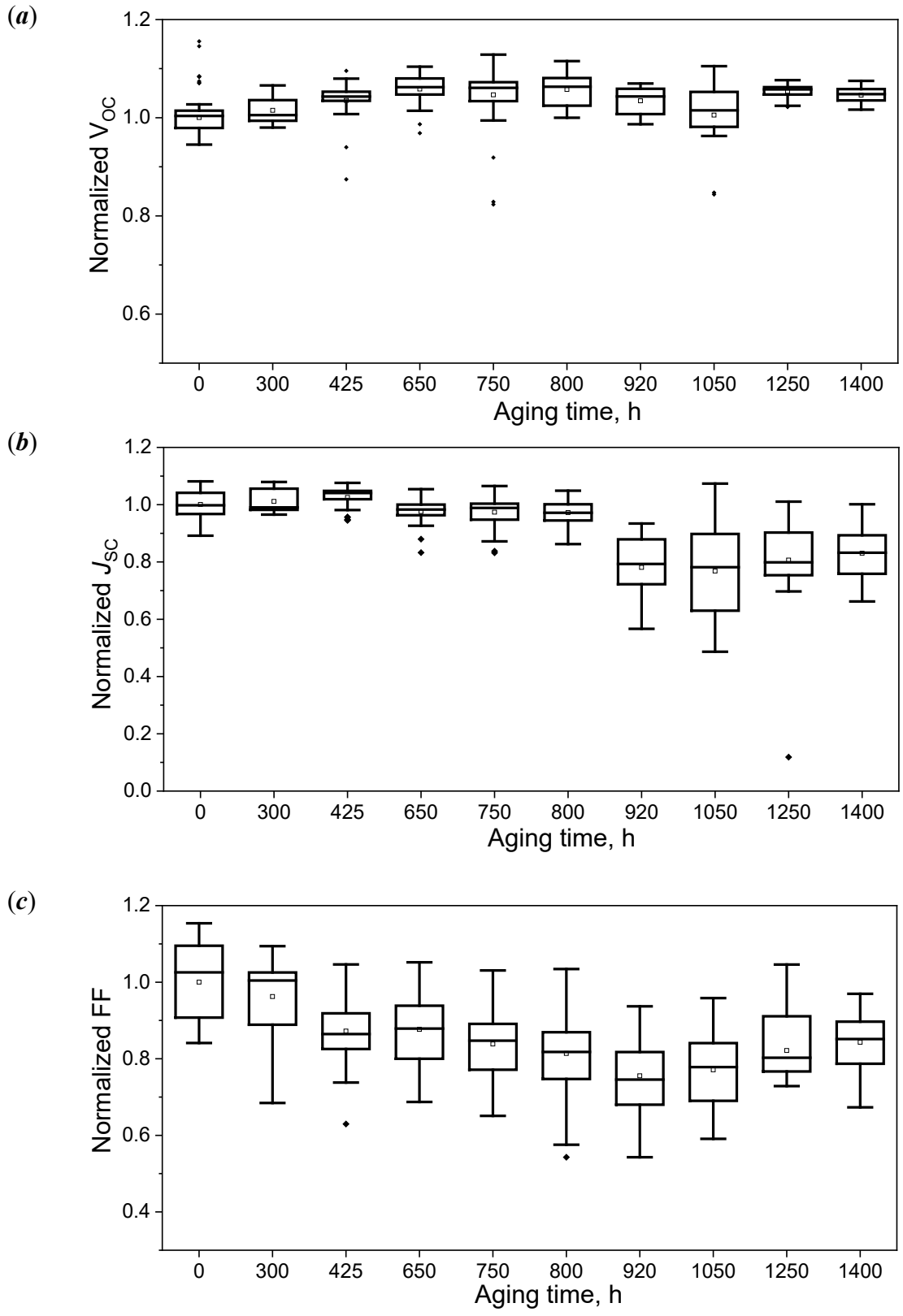

Figure S6. Evolution of the normalized open circuit voltage (V_{OC}) (***a***), short circuit current (J_{SC}) (***b***), and fill factor (FF) (***c***) values of the $CsPbI_3$+10% INPA devices upon h exposure to light (500±10 mW/cm^2, T = 35±2^{o}C).

Table S1. Optical absorption edges and bandgaps estimated from the Tauc plots for the $CsPbI_3$+x%INPA films with various compositions

Perovskite composition	**Absorption edge, nm / Bandgap, eV**
$CsPbI_3$	715 / 1.734
$CsPbI_3$+5% INPA	713 / 1.739
$CsPbI_3$+10% INPA	710 / 1.745
$CsPbI_3$+15% INPA	702 / 1.765
$CsPbI_3$+30% INPA	699 / 1.774

Table S2. PL peak positions for the $CsPbI_3$+x%INPA films with various compositions.

Perovskite composition	**PL peak position, nm**
$CsPbI_3$	695
$CsPbI_3$+5% INPA	706
$CsPbI_3$+10% INPA	703
$CsPbI_3$+15% INPA	694
$CsPbI_3$+30% INPA	687

Table S3. Average and the best (in brackets) values of power conversion efficiency (*PCE*), open-circuit voltage (V_{OC}), short-circuit current density (J_{SC}), and fill factor (*FF*) for devices with different INPA contents.*

INPA content, % mol.	V_{OC}, **mV**	J_{SC}, **mA cm^{-2}**	***FF*, %**	**PCE, %**
1	(890) 854 ± 28	(15.1) 14.3± 0.3	(48.1) 44.0 ± 1.5	(5.9) 5.7 ± 0.3
3	(960) 934 ± 25	(15.4) 14.7± 0.6	(51.6) 49.4± 1.4	(7.2) 6.8 ± 0.4
7	(1007) 957 ± 26	(16.3) 15.9 ± 0.4	(65.0) 61.6 ± 2.5	(10.0) 9.4 ± 0.4
10	(1135) 1076 ± 56	(16.0) 15.7 ± 0.3	(66.0) 63.7 ± 2.2	(12.0) 10.9 ± 1.1
12	(992) 942± 32	(15.8) 14.7 ± 0.9	(52.6) 43.2 ± 5.0	(7.4) 6.6 ± 0.7
15	(969) 891 ± 35	(2.7) 1.6 ± 0.4	(27.2) 25.5 ± 1.3	(0.6) 0.4 ± 0.1

Note: * The *J–V* curves were measured in reverse direction with a scan rate of 0.01 V/s.

References

S1. S. A. Adonin, L. A. Frolova, M. N. Sokolov, G. V. Shilov, D. V. Korchagin, V. P. Fedin, S. M. Aldoshin, K. J. Stevenson and P. A. Troshin, *Adv. Energy Mater*., 2018, **8**, 1701140.